Available online at www.sciencedirect.com

ScienceDirect

IFAC PapersOnline CONFERENCE PAPER ARCHIVE

IFAC PapersOnLine 56-1 (2023) 301–306

Frequency-domain stability conditions for split-path nonlinear systems

S.J.A.M. van den Eijnden * **B. Sharif** * **M. F. Heertjes** *
W.P.M.H. Heemels *

* *Eindhoven University of Technology, Department of Mechanical Engineering, Eindhoven, The Netherlands*

Abstract: This paper considers the class of control systems containing so-called split-path nonlinear (SPAN) filters, which are designed to overcome some of the well-known fundamental limitations in linear time-invariant (LTI) control. In this work, we are interested in developing tools for the stability analysis of such systems using frequency-domain techniques. Hereto, we explicitly show the equivalence between a set of linear matrix inequalities (LMIs) with S-procedure terms, guaranteeing stability of the closed-loop (SPAN) system, and a frequency-domain condition. We also provide a systematic procedure for verifying the frequency-domain condition in a graphical manner. The results are illustrated through a nummerical case study.

1. INTRODUCTION

Over the past decades, the desire of many researchers and practitioners to break away from the fundamental limitations of LTI control systems imposed by, *e.g.*, Bode's gain-phase relationship (Middleton et al., 1990), has led to the development of many nonlinear control strategies, including various reset and switching type controllers (Clegg , 1958; Beker et al., 2001; Feuer et al., 1997; van den Eijnden et al., 2020; Deenen et al., 2021). A particularly interesting strategy that was proposed in the late sixties by W.C. Foster and co-workers is the so-called split-path nonlinear (SPAN) filter (Foster et al., 1996). The key philosophy underlying this filter is to "split" the magnitude and phase characteristics of a linear filter as to design these separately with the intention to circumvent Bode's gain-phase relationship, thereby facilitating an additional degree-of-freedom in the controller design. Revived interest in this approach has recently led to an extension of the SPAN filter that includes integral action (van Loon et al., 2016; Sharif et al., 2022). This so-called filtered SPAN integrator (F-SPANI) aims for an improved integrator design, with all the benefits of an LTI integrator in terms of achieving zero steady-state tracking error, but without introducing phase lag. It was shown in (Sharif et al., 2022) that using a F-SPANI filter in an otherwise linear feedback controller can significantly improve transient performance properties of the closed-loop controlled system.

For asserting stability of a closed-loop system including a SPAN(I) filter, conditions have been proposed recently in Sharif et al. (2022) in the form of linear matrix inequalities (LMIs). Although such conditions can be verified by means of numerical methods, these require a parametric model of the plant. In many high-tech industrial applications that may benefit from the use of SPAN(I) filters, such as, *e.g.*, wafer scanners, pick-and-place machines, and atomic force microscopes, this sometimes is considered a drawback, as accounting for machine-to-machine variation in the parametric model description is not an easy task. Instead, for such applications frequency-domain-based tools may be preferred as these provide several distinct advantages over LMI-based methods. First, frequency-domain methods allow for exploiting non-parametric models obtained from *measured* frequency-response-function (FRF) data, which in many industrial contexts, is often easy to obtain. Second, such tools can be extended toward a robust stability analysis by including (un)structured plant uncertainty in a much more straightforward manner as compared to LMI methods, see, for instance, Tsypkin et al (1992). As a third advantage, in sharp contrast to LMI methods, frequency-domain conditions provide intuitive insight in how to redesign the controller when the conditions are violated. Moreover, these can be easily embedded into existing tools for LTI controller tuning, such as, *e.g.*, autotuners (Astrom et al., 2001), that allows for an (automated) controller tuning procedure. The latter interfaces well with current industrial practice that is dominated by frequency-domain loopshaping methods, and, therefore, frequency domain tools can speed up the adoption of SPAN (and other type of hybrid) controllers in practice.

Motivated by the numerous benefits of frequency-domain tools, in this paper we contribute to the development of such tools for the class of SPAN-controlled systems. In particular, we present the equivalence between a set of LMI conditions guaranteeing closed-loop stability, and a new frequency-domain condition. The latter can be checked entirely on the basis of experimentally obtained plant data in the form of FRF measurements. We make use of a result that was already published in the Russian control literature in 1983, see Kamenetskiy (1983), and has only recently been further exploited by the same author in Kamenetskiy (2017). Surprisingly, this result appears to be lesser known in the western literature.

In line with the above, the main contributions in this paper are as follows. First, we generalize the LMI conditions in Sharif et al. (2022) for stability analysis of SPAN-

* The research leading to these results has received funding from the European Research Council under the Advanced ERC Grant Agreement PROACTHIS, no. 101055384.

10.1016/j.ifacol.2023.02.051

controlled systems by including S-procedure relaxation terms. Second, we present the equivalence between feasibility of this set of LMIs and feasibility of a frequency-domain inequality. Third, we provide a systematic sequential procedure for verifying the frequency-domain inequality by using FRF data concerning the plant dynamics. As a by-product, we hope to bring the result in Kamenetskiy (1983) to the attention of the control community, as we believe it can provide a useful step in further developing "industry-friendly" tools for stability analysis of nonlinear/hybrid systems in frequency-domain.

The remaining part of this paper is outlined as follows. In Section 2 the SPAN filter, closed-loop system, and problem formulation are discussed. Section 3 presents the main results of this paper, which establishes a frequency-domain condition for proving stability of a SPAN-controlled system. Applicability and verification of this condition is demonstrated through a numerical example In Section 4. Finally, Section 5 presents the main conclusions.

Notation

A single-input single-output (SISO) transfer function is said to be stable if all its poles are located in the open left-half complex plane. The real and imaginary parts of a complex matrix $W \in \mathbb{C}^{n\times n}$ are denoted by $\mathrm{Re}\{W\} \in \mathbb{R}^{n\times n}$ and $\mathrm{Im}\{W\} \in \mathbb{R}^{n\times n}$, respectively, and thus $W = \mathrm{Re}\{W\} + i\mathrm{Im}\{W\}$, and the Hermitian transpose is indicated by W^*. The set of complex Hermitian matrices in $\mathbb{C}^{n\times n}$ is denoted by $\mathbb{S}^{n\times n}$. A symmetric matrix $P \in \mathbb{S}^{n\times n}$ is positive (negative) definite, denoted by $P \succ 0$ ($P \prec 0$), if $x^*Px > 0$ ($x^*Px < 0$) for all $x \in \mathbb{C}^n \setminus \{0\}$. We also make use of the notation $\mathrm{He}(P) = P + P^\top$.

2. SYSTEM DESCRIPTION

2.1 Split-path nonlinear (SPAN) filter

The class of nonlinear controllers considered in this work belong to the class of SPAN filters as shown in Fig. 1 and introduced in Foster et al. (1996) to facilitate independent tuning of gain and phase characteristics of a signal. As

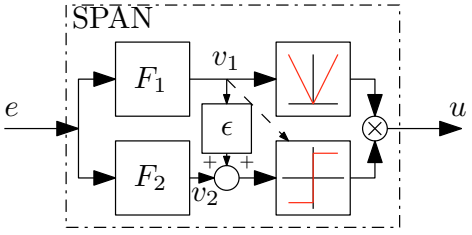

Fig. 1. SPAN filter.

shown in Fig. 1, the input signal e of a SPAN filter is split into two branches. The output of the filter is formed by multiplying the output of the two branches. The upper branch, referred to as the *magnitude branch*, retains all magnitude information and removes all sign information, *i.e.*, it outputs $|v_1|$. The lower branch on the other hand, referred to as the *sign branch*, retains all sign information and removes all magnitude information, *i.e.*, it outputs ± 1 depending on the sign of its input. Moreover, each branch has a linear filter F_i, $i \in \{1, 2\}$, which can be used to shape

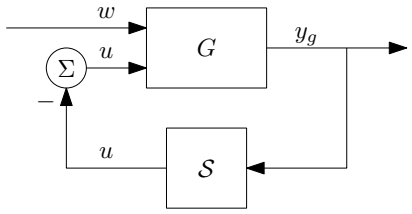

Fig. 2. SPAN-controlled closed-loop system.

the amplitude and phase characteristics of the overall SPAN filter independently. The SPAN *integrator* as in Sharif et al. (2022); van Loon et al. (2016), being a specific type of the generic SPAN filter in Foster et al. (1996) can for example be constructed by choosing $F_1(s) = 1/s$ and $F_2(s) = 1$. The generic SPAN filter is described by

$$\mathcal{S}: \begin{cases} F_i: & \begin{cases} \dot{x}_i(t) = \mathcal{A}_i x_i(t) + \mathcal{B}_i e(t), \\ v_i(t) = \mathcal{C}_i x_i(t) + \mathcal{D}_i e(t), \end{cases} \\ u(t) = & \begin{cases} v_1(t), & \text{if } \varphi(t) \geq 0, \\ -v_1(t), & \text{if } \varphi(t) \leq 0 \end{cases} \end{cases} \tag{1}$$

with $x_i(t) \in \mathbb{R}^{n_i}$, $e(t) \in \mathbb{R}$, $v_i(t) \in \mathbb{R}$, $i \in \{1, 2\}$, denoting the state, input and output of Filter F_i at time $t \in \mathbb{R}_{\geq 0}$, respectively, and where $\varphi(t) := v_1(t)(v_2(t) + \epsilon v_1(t))$. Moreover, $u(t) \in \mathbb{R}$ denotes the output of the SPAN filter at time $t \in \mathbb{R}_{\geq 0}$ and $\mathcal{A}_i, \mathcal{B}_i, \mathcal{C}_i, \mathcal{D}_i$, $i \in \{1, 2\}$, are all real matrices of appropriate dimensions. Lastly, $\epsilon > 0$ is a tuning parameter. As described in (1), the output of the SPAN filter is determined based on the sign of $\varphi(t)$. In particular, the filter outputs $v_1(t)$ when $\varphi(t) \geq 0$ and $-v_1(t)$ when $\varphi(t) \leq 0$. We refer to the system (1) as being in mode 1 when $u(t) = v_1(t)$, and as being in mode 2 when $u(t) = -v_1(t)$. The parameter ϵ has been included for robustness purposes with respect to slight perturbations around desired equilibrium of the system satisfying $e = 0$, see van Loon et al. (2016); Sharif et al. (2022) for details.

2.2 Closed-loop system description

In this paper, we consider the closed-loop system as in Fig. 2 consisting of an LTI system G and a SPAN filter $\mathcal{S}$, the latter as described in (1). Here, G contains the linear part of the loop consisting of the plant to be controlled and, possibly, linear control elements and is described by

$$G: \begin{cases} \dot{x}_g(t) &= A_g x_g(t) + B_{gv} u(t) + B_{gw} w(t) \\ y_g(t) &= C_g x_g(t), \end{cases} \tag{2}$$

where $x_g(t) \in \mathbb{R}^n$ are the plant states, $w(t) \in \mathbb{R}^m$ are the external inputs (*e.g.*, set-points or disturbances), $u(t) \in \mathbb{R}$ is the output of the SPAN filter, and $y_g(t) \in \mathbb{R}$ is the output of the plant at time $t \in \mathbb{R}_{\geq 0}$. Combining (2) and (1), we obtain the switched linear description

$$\dot{x}(t) = \begin{cases} A_1 x(t) + B w(t), & \text{if } \varphi(t) \geq 0, \\ A_2 x(t) + B w(t), & \text{if } \varphi(t) \leq 0 \end{cases} \tag{3}$$

with $x = [x_g^\top \ x_1^\top \ x_2^\top]^\top$, where x_1, x_2 denote the states of the filters F_1 and F_2 in (1), respectively, and

$$\begin{aligned} A_1 &= \begin{bmatrix} A_g - B_{gv}\mathcal{D}_1 C_g & -B_{gv}\mathcal{C}_1 & 0 \\ \mathcal{B}_1 C_g & \mathcal{A}_1 & 0 \\ \mathcal{B}_2 C_g & 0 & \mathcal{A}_2 \end{bmatrix}, \\ A_2 &= \begin{bmatrix} A_g + B_{gv}\mathcal{D}_1 C_g & B_{gv}\mathcal{C}_1 & 0 \\ \mathcal{B}_1 C_g & \mathcal{A}_1 & 0 \\ \mathcal{B}_2 C_g & 0 & \mathcal{A}_2 \end{bmatrix}, \quad B = \begin{bmatrix} B_{gw} \\ 0 \\ 0 \end{bmatrix}. \end{aligned} \tag{4}$$

Note that the matrices A_1 and A_2 differ by a rank 1 matrix according to $A_1 - A_2 = -2bC_1$, with $b = \begin{bmatrix} B_{gv}^\top & 0_{n_1+n_2} \end{bmatrix}^\top$, and $C_1 = [\mathcal{D}_1 C_g \ \mathcal{C}_1 \ 0]$. This property of the closed-loop system will be key for proving our main results.

Solutions to (3) will be considered in the sense of Filippov (Fillipov, 1998). In particular, we define solutions as locally absolutely continuous functions satisfying the differential inclusion

$$\dot{x} \in D(x) := \begin{cases} \{A_1 x + Bw\}, & \text{if } \varphi > 0, \\ \text{co}(A_1 x, A_2 x) + Bw, & \text{if } \varphi = 0, \\ \{A_2 x + Bw\}, & \text{if } \varphi < 0, \end{cases} \tag{5}$$

almost everywhere, as solutions to the closed-loop system. Here, $\text{co}(A_1 x, A_2 x)$ denotes the convex hull $\{\lambda A_1 x + (1-\lambda)A_2 x, \ \lambda \in [0,1]\}$. This Fillipov solution concept allows for the convex combination of the vector fields in (3) to be active in the region described by $\varphi = v_1(v_2 + \epsilon v_1) = 0$, and thus allows for possible sliding modes.

2.3 Problem formulation

This paper is concerned with formulating conditions for stability of the closed-loop system in (5). Stability is studied through the notion of input-to-state stability (ISS), as presented in, *e.g.*, Khalil (2002).

The next theorem presents sufficient conditions in the form of LMIs for guaranteeing ISS of (5). It essentially provides a generalization of the LMI-based conditions presented in Sharif et al. (2022) by including S-procedure terms.

Theorem 1. *The differential inclusion in* (5) *is ISS if there exist a positive definite matrix* $P = P^\top \succ 0$ *and a number* $\tau \geq 0$ *satisfying*

$$A_1^\top P + P A_1 + \left(S + S^\top\right) \prec 0, \tag{6}$$

$$A_2^\top P + P A_2 - \tau \left(S + S^\top\right) \prec 0, \tag{7}$$

in which $S = C_1^\top(\epsilon C_1 + C_2)$ *with* $C_1 = [\mathcal{D}_1 C_g \ \mathcal{C}_1 \ 0]$, *and* $C_2 = [\mathcal{D}_2 C_g \ 0 \ \mathcal{C}_2]$.

Proof. The proof largely proceeds along the steps of the proof of (Sharif et al., 2022, Theorem 1), with the addition of S-procedure terms. Regarding the convex combination of the dynamics in (5), note that these happen on a lower-dimensional region satisfying $v_1(v_2 + \epsilon v_1) = 0$, which on the level of the state x, translates to $x^\top C_1^\top(\epsilon C_1 + C_2)x = x^\top S x = 0$. Finsler's lemma is used to show that

$$\text{He}\left(x^\top P \left(\lambda A_1 + (1-\lambda)A_2\right) x\right) \prec 0, \tag{8}$$

for all x satisfying $x^\top(S + S^\top)x = 0$ and all $\lambda \in [0,1]$. □

Although the LMIs in (6), (7) are numerically tractable, solving them requires a state-space model, which may be hard to obtain in practical applications if one desires an accurate, machine-specific, model description. Moreover, the conditions provide limited insight in the (re)design of controllers for guaranteed stability when the LMIs turn out to be infeasible. Motivated by these concerns, the main objective in this paper is to establish the equivalence between feasibility of the LMIs in (6), (7), and frequency-domain conditions that exploit non-parametric models, thereby allowing a transition from time- to frequency-domain conditions for guaranteeing ISS of (5), and abandoning the need for parametric models.

3. FREQUENCY-DOMAIN CONDITIONS

To derive new frequency-domain conditions for ISS, we will start with some preparatory results.

3.1 Preliminary results

Typical frequency-domain conditions for guaranteeing the existence of a Lyapunov function for a piecewise linear system such as in (5) make use of the Kalman-Yakubovich-Popov (KYP) lemma and require the evaluation of some *stable* transfer function, see, *e.g.*, Khalil (2002). However, due to the use of the S-procedure relaxation terms in Theorem 1, the system matrices A_1 and A_2 as in (4), and thus the associated transfer functions do not need to be stable. For our results, the following lemma is essential.

Lemma 1. *Feasibility of the LMIs in* (6), (7) *for some* $P = P^\top \succ 0$, *and* $\tau \geq 0$ *imply feasibility of the inequality*

$$A_0^\top P + P A_0 \prec 0, \quad \text{with} \quad A_0 = A_2 + 2\alpha b C_1, \tag{9}$$

$b = \begin{bmatrix} B_{gv}^\top & 0_{n_1+n_2} \end{bmatrix}^\top$, $C_1 = [\mathcal{D}_1 C_g \ \mathcal{C}_1 \ 0]$, *and* $\alpha = \tau/(1+\tau)$.

Proof. When (6) and (7) are satisfied, their convex combination satisfies for all $\alpha \in [0,1]$

$$\text{He}\{P(\alpha A_1 + (1-\alpha)A_2)\} + (\alpha - \tau(1-\alpha))(S + S^\top) \prec 0.$$

Since the matrices A_1 and A_2 in (3) satisfy $A_1 = A_2 + 2bC_1$, the result follows for $\alpha = \tau/(1+\tau) \in [0,1)$. □

The next lemma recalls the key result from Kamenetskiy (2017), that is instrumental in proving the main result.

Lemma 2 (Kamenetskiy (2017))**.** *To satisfy a system of two matrix inequalities*

$$I_1 \prec 0, \quad I_2 \prec 0, \tag{10}$$

for which the difference satisfies $I_2 - I_1 = pq^\top + qp^\top$ *with vectors* $p, q \in \mathbb{R}^n$, *it is necessary and sufficient that there exists a number* $\varepsilon > 0$ *such that the inequality*

$$I_1 + Q^+(\varepsilon) = I_2 + Q^-(\varepsilon) \prec 0, \tag{11}$$

with

$$Q^\pm(\varepsilon) = \left(\frac{\varepsilon}{\sqrt{2}} p \pm \frac{1}{\varepsilon\sqrt{2}} q\right)\left(\frac{\varepsilon}{\sqrt{2}} p \pm \frac{1}{\varepsilon\sqrt{2}} q\right)^\top \tag{12}$$

is satisfied.

It has been shown in Kamenetskiy (1983) that a system of N inequalities can be reduced into a single (equivalent) inequality by applying Lemma 2 repeatedly to each pair of inequalities from the original system whose difference is of the form $pq^\top + qp^\top$, see Kamenetskiy (1983) for more details regarding this statement. This principle will be applied in proving the main theorem of the next section.

3.2 Main result

Equipped with the above results and definitions, we are now ready to provide the main result of this paper.

Theorem 2. *Consider the closed-loop system in* (5). *The following statements are equivalent:*

- *The set of LMIs in* (6), (7) *is feasible for some* $P = P^\top \succ 0$, *and* $\tau \geq 0$;

- *There exist numbers $\tau \geq 0$, $\gamma \in (-1,1)$, and $\varepsilon_i > 0$, $i = 1,2$, such that the matrix $A_0 := A_2 + 2\frac{\tau}{1+\tau} bC_1$ is Hurwitz, and the frequency-domain inequality*

$$2\Gamma^{-1} - (W(j\omega)M + MW^*(j\omega)) \succ 0, \tag{13}$$

with $W(j\omega) = \operatorname{diag}\{[W_1(j\omega), W_2(j\omega)]\} \in \mathbb{C}^{2\times 2}$, in which

$$W_1(j\omega) = \left(H - \frac{1}{\varepsilon_1^2}C_1\right)(j\omega I - A_0)^{-1}b \tag{14}$$

$$W_2(j\omega) = \left(H + \frac{1}{\varepsilon_2^2}C_1\right)(j\omega I - A_0)^{-1}b, \tag{15}$$

and where

$$M = \frac{1}{1+\tau}\begin{bmatrix} \varepsilon_1^2 & \varepsilon_1\varepsilon_2\sqrt{\tau} \\ \varepsilon_1\varepsilon_2\sqrt{\tau} & \varepsilon_2^2\tau \end{bmatrix}, \quad \Gamma^{-1} = \begin{bmatrix} 1 & \gamma \\ \gamma & 1 \end{bmatrix},$$

$H = \epsilon C_1 + C_2$, is satisfied for all $\omega \in \mathbb{R} \cup \{\infty\}$.

Proof. By virtue of Lemma 1, one finds that feasibility of (6), (7) is equivalent to feasibility of (6), (7), and (9). Note that we do not directly apply Lemma 2 to (6) and (7). In fact, the application of Lemma 1 is crucial in the construction below as it allows to obtain LMI conditions in terms of the Hurwitz matrix A_0 which can in turn be translated to frequency-domain conditions by virtue of the KYP Lemma. Next, observe that the difference between the inequalities in (9) (which will be denoted by $I_0 \prec 0$) and (6) (which will be denoted by $I_1 \prec 0$) reads as

$$I_1 - I_0 = \left(2kPb + H^\top\right)C_1 + C_1^\top\left(2kPb + H^\top\right)^\top \tag{16}$$

with $k = 1/(1+\tau)$ and $H = \epsilon C_1 + C_2$. Applying Lemma 2 to I_0 and I_1 with $p = 2kPb + H^\top$ and $q = C_1^\top$ shows that feasibility of these two inequalities is equivalent to feasibility of the single inequality

$$A_0^\top P + PA_0 + U_1U_1^\top \prec 0 \tag{17}$$

with

$$U_1 = \left(\frac{\varepsilon_1}{\sqrt{2}}\left(2kPb + H^\top\right) - \frac{1}{\varepsilon_1\sqrt{2}}C_1^\top\right) \tag{18}$$

for some $\varepsilon_1 > 0$. Through similar steps, one finds that feasibility of (9) (denoted by $I_0 \prec 0$) and (7) (denoted by $I_2 \prec 0$) is equivalent to feasibility of the single inequality

$$A_0^\top P + PA_0 + U_2U_2^\top \prec 0 \tag{19}$$

with

$$U_2 = \sqrt{\tau_2}\left(\frac{\varepsilon_2}{\sqrt{2}}\left(2kPb + H^\top\right) + \frac{1}{\varepsilon_2\sqrt{2}}C_1^\top\right) \tag{20}$$

for some $\varepsilon_2 > 0$. At this point, we have only shown that feasibility of the LMIs in (6) and (7) is equivalent to feasibility of the inequalities in (17) and (19). The reason for taking this intermediate step is that (17) and (19) now contain the Hurwitz matrix A_0, which allows directly for converting the inequalities into frequency-domain conditions. In order to proceed, we apply Lemma 2 one more time to the inequalities in (17) (denoted by $I_1' \prec 0$) and (19) (denoted by $I_2' \prec 0$). The difference between I_2' and I_1' can be written as

$$I_2' - I_1' = U_2U_2^\top - U_1U_1^\top = uv^\top + vu^\top$$

with

$$u = \frac{1}{\sqrt{2}}(U_2 + U_1), \quad \text{and} \quad v = \frac{1}{\sqrt{2}}(U_2 - U_1). \tag{21}$$

By Lemma 2, feasibility of (17), (19) is then equivalent to feasibility of the single inequality

$$A_0^\top P + PA_0 + U_2U_2^\top + U_3U_3^\top \prec 0 \tag{22}$$

with

$$U_3 = \left(\frac{\varepsilon_3}{\sqrt{2}}u - \frac{1}{\varepsilon_3\sqrt{2}}v\right), \tag{23}$$

for some $\varepsilon_3 > 0$. Note that we can write $U_2U_2^\top + U_3U_3^\top = U\Gamma U^\top$ with $U = [U_1\ U_2]$, and

$$\Gamma = \frac{1}{4}\begin{bmatrix} 2 + \varepsilon_3^2 + \frac{1}{\varepsilon_3^2} & \varepsilon_3^2 - \frac{1}{\varepsilon_3^2} \\ \varepsilon_3^2 - \frac{1}{\varepsilon_3^2} & 2 + \varepsilon_3^2 + \frac{1}{\varepsilon_3^2} \end{bmatrix} \tag{24}$$

such that (22) can be written compactly as

$$A_0^\top P + PA_0 + U\Gamma U^\top \prec 0. \tag{25}$$

A simple calculation reveals that $\det(\Gamma) = 2 + \varepsilon_3^2 + \frac{1}{\varepsilon_3^2} > 0$, and thus the matrix Γ is non-singular, and, therefore, invertible. Applying Schur's Lemma to (25) yields

$$\begin{bmatrix} A_0^\top P + PA_0 & \sqrt{2}PY \\ \sqrt{2}Y^\top P & 0 \end{bmatrix} + Q \prec 0, \tag{26}$$

in which $Y = \begin{bmatrix} k\varepsilon_1 b & k\varepsilon_2\sqrt{\tau}b \end{bmatrix}$, and where

$$Q = \begin{bmatrix} 0 & \frac{1}{\sqrt{2}}F \\ \frac{1}{\sqrt{2}}F^\top & -\Gamma^{-1} \end{bmatrix}, \quad F^\top = \begin{bmatrix} \varepsilon_1 H - \frac{1}{\varepsilon_1}C_1 \\ \sqrt{\tau}\varepsilon_2 H + \frac{\sqrt{\tau}}{\varepsilon_2}C_1 \end{bmatrix}.$$

From the KYP lemma (Rantzer., 1996, Theorem 1), and the fact that A_0 is Hurwitz, (26) is equivalent to

$$\begin{bmatrix} (j\omega I - A_0)^{-1}Y \\ I \end{bmatrix}^* Q \begin{bmatrix} (j\omega I - A_0)^{-1}Y \\ I \end{bmatrix} \prec 0 \tag{27}$$

for all $\omega \in \mathbb{R} \cup \{\infty\}$, which evaluates to

$$2\Gamma^{-1} - (W(j\omega)M + MW^*(j\omega)) \succ 0, \tag{28}$$

with $W(j\omega)M = F^\top(j\omega I - A_0)^{-1}Y \in \mathbb{C}^{2\times 2}$. Note that

$$\Gamma^{-1} = \begin{bmatrix} 1 & \gamma \\ \gamma & 1 \end{bmatrix} \quad \text{with} \quad \gamma = \frac{1 - \varepsilon_3^2}{1 + \varepsilon_3^2}. \tag{29}$$

and clearly $\gamma \in (-1,1)$. Hence, in summary, feasibility of (28) is equivalent to feasibility of (26), which, in turn, is equivalent to feasibility of (6), (7). □

4. VERIFYING THE CONDITIONS

At this point, verifying the frequency-domain inequality in (13) may appear a cumbersome task due to the nonlinear combination of the stability parameters $\tau, \varepsilon_1, \varepsilon_2$, and γ. Of course, one can make some simplifying assumptions. For example, setting $\varepsilon_1 = \varepsilon_2 = 1$ could lead to more tangible conditions, but at the cost of loosing necessity. To avoid this, in this section we will propose a sequential procedure for finding the parameters $\tau, \varepsilon_1, \varepsilon_2, \gamma$ (if they exist). We will illustrate the use of each step in the procedure through a numerical example, in which the plant is given by

$$G(s) = \frac{1}{s^2 + 0.25s + 8}, \tag{30}$$

and the SPAN filter is described by

$$F_1(s) = \frac{2}{s + 0.7}, \quad F_2(s) = 1, \text{ and } \epsilon = 10^{-6}. \tag{31}$$

This SPAN filter has similar characteristics as a (weak) integrator (or low-pass filter) but aims at reducing the phase lag that is normally induced by its LTI counterpart.

Before presenting the steps in the procedure, however, we first dissect the frequency-domain condition in (13) into several more tangible sub-conditions.

4.1 Dissecting the conditions

For verifying the frequency-domain conditions in Theorem 2 we essentially need to verify both stability of the matrix A_0, and positive definiteness of the 2×2 Hermitian matrix $2\Gamma^{-1} - (W(j\omega)M + MW^*(j\omega))$. The latter can be done by verifying if the diagonal elements and determinant of this matrix are strictly positive. This results in the following necessary and sufficient conditions to be satisfied:

(1) The existence of $\tau \geq 0$ such that the matrix $A_0 = A_2 + 2\frac{\tau}{1+\tau}bC_1$ is Hurwitz;
(2) The existence of $\tau \geq 0$ and $\varepsilon_1 > 0$ such that
$$M_1 := \frac{1}{k} - \mathrm{Re}\left\{(\varepsilon_1^2 H - C_1)(j\omega I - A_0)^{-1}b\right\} > 0 \quad (32)$$
is satisfied;
(3) The existence of $\tau \geq 0$ and $\varepsilon_2 > 0$ such that
$$M_2 := \frac{1}{\tau k} - \mathrm{Re}\left\{(\varepsilon_2^2 H + C_1)(j\omega I - A_0)^{-1}b\right\} > 0 \quad (33)$$
is satisfied;
(4) The existence of $\tau \geq 0, \varepsilon_1 > 0, \varepsilon_2 > 0$, and $\gamma \in (-1, 1)$ such that
$$M_1 M_2 - (\gamma - \sqrt{\tau}\varepsilon_1\varepsilon_2\Lambda_1)^2 - \left(\sqrt{\tau}\varepsilon_1\varepsilon_2\Lambda_2\right)^2 > 0, \quad (34)$$
with
$$\Lambda_1 = \mathrm{Re}\left\{\left(H + \left(\frac{1}{\varepsilon_2^2} - \frac{1}{\varepsilon_1^2}\right)C_1\right)(j\omega I - A_0)^{-1}b\right\},$$
$$\Lambda_2 = \mathrm{Im}\left\{\left(\frac{1}{\varepsilon_2^2} + \frac{1}{\varepsilon_1^2}\right)C_1(j\omega I - A_0)^{-1}b\right\},$$
is satisfied.

The second and third item correspond to the diagonal entries of the matrix $2\Gamma^{-1} - (WM + MW^*)$ being positive; the fourth item shows its determinant to be positive.

We make the following essential observation. The above items sequentially depend on the stability parameters, *i.e.*, the first item only requires the value of τ, the second item requires τ and ε_1 and so on. This aspect allows for formulating a sequential procedure.

4.2 Sequential procedure

The proposed sequential procedure consists of three steps.

Step 1. In the first step, the parameter $\tau \geq 0$ is searched for that renders the matrix $A_0 = A_2 - 2kbC_1$ with $k = \tau/(1+\tau)$ Hurwitz. Note that this test essentially requires the feedback interconnection of the LTI system $L(j\omega) = 2C_1(j\omega I - A_2)^{-1}b$ and a negative feedback gain k to be stable. This can be verified graphically by means of the well-known Nyquist stability test. The admissible range for k, and thus for τ is limited by the gain-margin of the system L. For the example in (30), (31) we need to check stability through the loop characteristics [1]
$$L(j\omega) = \frac{2P(j\omega)F_1(j\omega)}{(1 - F_1(j\omega)P(j\omega))}.$$
The Nyquist plot of L is shown in Fig. 3, and demonstrates that the admissible feedback gain is given by $k \in (0, 1.042)$.

[1] Stability of L itself can be verified via a Nyquist plot of $\tilde{L}(j\omega) = P(j\omega)F_1(j\omega)$. Note that P and F_1 both are stable as well.

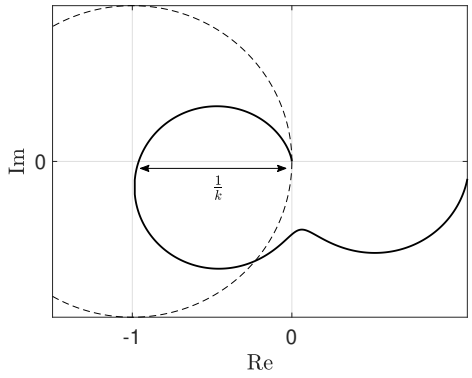

Fig. 3. Nyquist test for finding $k = \tau/(1+\tau)$.

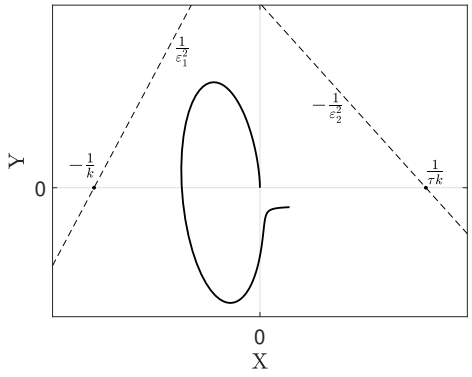

Fig. 4. Popov-like test for finding ε_1, and ε_2.

Step 2. Select an admissible value for τ as obtained in Step 1. For the example, we pick $k = 0.5$, which yields $\tau = 1$. Next, the parameters $\varepsilon_1 > 0$ and $\varepsilon_2 > 0$ that satisfy (32) and (33) are searched for. This can be done graphically as follows. Define $X(j\omega) := \mathrm{Re}\left\{C_1(j\omega I - A_0)^{-1}b\right\}$ and $Y(j\omega) := \mathrm{Re}\left\{H(j\omega I - A_0)^{-1}b\right\}$. Then, the inequality in (32) is satisfied if the Nyquist plot of $\mathcal{G} := X + iY$ remains to the *right* of a straight line that passes through the point $(-1/k, 0)$ and has a slope of $1/\varepsilon_1^2$. This graphical test somewhat resembles the classical Popov-plot (Khalil, 2002, Section 7.1), and provides an admissible range for ε_1. The inequality in (33) can be verified in a similar manner. That is, the Nyquist plot of $\mathcal{G}$ must remain to the *left* of a straight line that passes through the point $(1/(\tau k), 0)$ and has a slope of $-1/\varepsilon_2^2$, thereby providing an admissible range for the values of ε_2. Note that the Nyquist plot of $\mathcal{G}$ should thus remain within the cone spanned by the aforementioned straight lines. For the example in (30), (31) we find $X(j\omega) = \mathrm{Re}\{F_1(j\omega)P(j\omega)S(j\omega)\}$, and $Y(j\omega) = \mathrm{Re}\{(1 + \epsilon F_1(j\omega))P(j\omega)S(j\omega)\}$, where
$$S(j\omega) = \frac{1}{1 + kL(j\omega)}.$$
An illustration of this Popov-like test is shown for the example in (30), (31) in Fig. 4 with $\varepsilon_1 = 1$, and $\varepsilon_2 = 1.3$. Note that we allow a deliberate margin for the purpose of satisfying the remaining conditions.

Step 3. Fix the values for $\tau, \varepsilon_1, \varepsilon_2$ as obtained in the previous steps. Recall that for the running example we have $\tau = 1$, $\varepsilon_1 = 1$, and $\varepsilon_2 = 1.3$. Next, the parameter

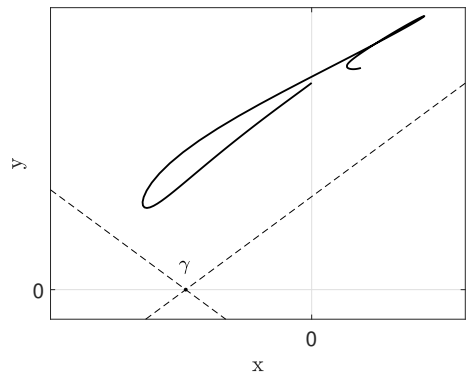

Fig. 5. Conic test for finding γ.

$\gamma \in (-1, 1)$ is searched for that satisfies (34). First note that for (34) to be satisfied it is necessary that $M_1 M_2 - (\sqrt{\tau}\varepsilon_1\varepsilon_2\Lambda_2)^2 > 0$. If this condition is not satisfied for the chosen values of $\tau, \varepsilon_1, \varepsilon_2$, then one should start with different values. Otherwise, define $x := -\sqrt{\tau}\varepsilon_1\varepsilon_2\Lambda_1$ and $y := \sqrt{M_1 M_2 - (\sqrt{\tau}\varepsilon_1\varepsilon_2\Lambda_2)^2}$ such that (34) can be written more compactly as

$$y^2 - (\gamma - x)^2 > 0. \tag{35}$$

The equation $y^2-(\gamma-x)^2 = 0$ partitions the (x, y)-plane in four regions, spanned by the vectors $\pm[1, -1]$ and $\pm[1, 1]$. In x-direction, these regions are shifted by γ. Hence, if one can find a $\gamma \in (-1, 1)$ such that the Nyquist plot of $g := x + iy$ remains above (note that $y = \mathrm{Im}\{g\} > 0$) the conic region spanned by the vectors $[1, 1]$, $[1, -1]$ with the apex located at the point $(\gamma, 0)$, then (34) is satisfied. For the running example, we find

$$\begin{aligned}
M_1 &= \frac{1}{k} - \varepsilon_1^2 \mathrm{Re}\{(1 + \epsilon F_1)PS\} + \mathrm{Re}\{F_1 PS\}, \\
M_2 &= \frac{1}{\tau k} - \varepsilon_2^2 \mathrm{Re}\{(1 + \epsilon F_1)PS\} - \mathrm{Re}\{F_1 PS\}, \\
\Lambda_1 &= \mathrm{Re}\{(1 + \epsilon F_1)PS\} + \left(\frac{1}{\varepsilon_1^2} - \frac{1}{\varepsilon_2^2}\right) \mathrm{Re}\{F_1 PS\}, \\
\Lambda_2 &= \left(\frac{1}{\varepsilon_1^2} + \frac{1}{\varepsilon_2^2}\right) \mathrm{Im}\{F_1 PS\},
\end{aligned}$$

where for brevity dependence on $j\omega$ is omitted. The "conic" test is depicted in Fig. 5, and is satisfied for $\gamma = 0.9$. Since the last test is verified, we can conclude that the SPAN-controlled system (30), (31) is ISS.

5. CONCLUSIONS

In this paper, we have derived frequency-domain conditions for ISS of SPAN-controlled systems. Different from LMI-based tools, frequency-domain tools offer the use of non-parametric models. Moreover, such conditions easily allow for robustness measures against (un)structured plant uncertainty and can also be integrated in software solutions that are available for LTI control tuning. All these aspects are considered to be advantageous from an industrial perspective. Moreover, such conditions can be verified by graphical tests. In deriving the frequency-domain conditions, we started with sufficient LMI-based conditions for ISS. Use is made of the result in Kamenetskiy (1983) as well as KYP lemma by which the equivalence between these LMIs and a frequency-domain condition is shown, through a well-chosen intermediate step. We hope to further bring Kamenetskiy (1983) to the attention of the control community, as we believe it to be a valuable asset in developing practically useful tools for stability analysis of nonlinear/hybrid systems using frequency-domain techniques as a basis.

REFERENCES

R.H. Middleton, G.C. Goodwin, *Digital control and estimation. A unified approach*, Prentice Hall, 1990.

J.C. Clegg, 'A nonlinear integrator for servomechanisms', *Trans. Amer. Inst. Elect. Eng. II: Appl. Ind.*, 77(1), pp. 41-42, 1958.

O. Beker, C.V. Hollot, and Y. Chait, 'Plant with integrator: An example of reset control overcoming limitations of linear feedback', *IEEE Trans. Autom. Control*, 46(11), pp. 1797-1799, 2001.

A. Feuer, G.C. Goodwin, and M. Salgado, "Potential benefits of hybrid control for linear time invariant plants", in Proceedings of the 1997 American Control Conference, 5, pp. 2790-2794, 1997.

S. van den Eijnden, M. F. Heertjes, W. P. M. H. Heemels and H. Nijmeijer (2020). Hybrid Integrator-Gain Systems: A Remedy for Overshoot Limitations in Linear Control?, in IEEE Cont. Sys. Lett., 4(4), pp. 1042-1047.

D.A. Deenen, and B. Sharif, and S. van den Eijnden, and H. Nijmeijer, and W.P.M.H. Heemels, and M.F. Heertjes, " Projection-based integrators for improved motion control: Formalization, well-posedness and stability of hybrid integrator-gain systems", Automatica, 133, 2021.

W. C. Foster, D. L. Gieseking, and W. K. Waymeyer, "A nonlinear filter for independent gain and phase (with applications)", Trans. ASME J. Basic Eng., 88(2), pp. 457–462, 1966.

B. Sharif, A. van der Maas, N. van de Wouw, and W.P.M.H. Heemels, "Filtered Split-Path Nonlinear Integrator: A Hybrid Controller for Transient Performance Improvement", IEEE Trans. on Contr. Sys. Tech., 30(2), pp. 451-463, 2022.

Y.Z. Tsypkin, and B.T. Polyak, 'Robust Absolute Stability of Continuous Systems', *Int. Journal of Robust and Nonlin contr.*, 3(3), pp. 321-239, 1992.

K. Astrom, and K.T. Hagglund, "The future of PID control", Control Engineering Practice (PID Control), 9(11), pp. 1163-1175, 2001.

V.A. Kamenetskiy, Absolute stability and absolute instability of control systems with several nonlinear nonstationary elements, Aut. and Rem. Cont., 12, pp. 20-30, 1983.

V.A. Kamenetskiy, Frequency-Domain Stability Conditions for Hybrid Systems, Automation and Remote Control, 78(12), pp. 2101-2119, 2017.

S.J.L.M. van Loon, B.G.B. Hunnekens, W.P.M.H. Heemels, N. van de Wouw, and H. Nijmeijer, "Split-path nonlinear integral control for transient performance improvement", Automatica, 66, pp. 262-270, 2016.

A.F. Filippov, "Differential equations with discontinuous right hand sides", Mathematics and Its Applications Book Series, Springer, 1988.

H.K. Khalil, *Nonlinear Systems (3rd ed.)*, Prentice Hall, Upper Saddle River, New Jersey, 2002.

A. Rantzer, "On the Kalman-Yakubovich-Popov lemma", Systems & Control Letters, 28(1), pp. 7-10, 1996.